

On Collective Effects in Cavity Quantum Electrodynamics

Bo-Sture K. Skagerstam*

*Department of Physics,
The Norwegian University of Science and Technology,
N-7491 Trondheim, Norway[†]*

and

*Microtechnology Center at Chalmers MC2,
Department of Microelectronics and Nanoscience,
Chalmers University of Technology and Göteborg University,
S-412 96, Göteborg, Sweden*

We investigate the role of collective effects in the micromaser system as used in various studies of the physics of cavity electrodynamics. We focus our attention on the effect on large-time correlations due to multi-atom interactions. The influence of detection efficiencies and collective effects on the appearance of trapping states at low temperatures is also found to be of particular importance.

PACS numbers 32.80.-t, 42.50.-p, 42.50.Ct

I. INTRODUCTION

The idealized system of a two-level atom interacting with a second quantized single-mode electromagnetic field, confined in a cavity, plays an important role in the study of various fundamental aspects of quantum mechanics. The micromaser is a remarkable experimental realization of such a simple but fundamental system (for reviews and references see e.g. [1]). It is therefore also an example of one of the rare systems in Nature which exhibit a rich structure of physics that can be investigated experimentally and which, at the same time, can be studied by exact theoretical methods. In the optical regime a microlaser has also been realized experimentally [2]. Recently this has also been achieved for a one-atom system [3].

Many features of the micromaser system can be regarded to be of general interest. Various aspects of stochastic resonance has e.g. been explored in this system [4]. The micromaser also illustrates a feature of non-linear dynamical systems: turning on randomness may lead to an increase of the signal to noise ratio [5, 6]. It can, furthermore, be argued that the micromaser system is a simple illustration of the conjectured topological origin of second-order phase transitions [6, 7]. Trapping states [8, 9] have been generated in the stationary state of the micromaser system and therefore the generation of states with no classical analogue in such a system is feasible [10, 11]. A basic ingredient of the micromaser is the description of the dynamics in terms of the Dicke model [12] in the so called rotating wave approximation, i.e. the Jaynes-Cummings (JC) model [13]. Early experimental studies involves a confirmation of the JC-model predicted atom revivals [14]. Recently one has

also explicitly demonstrated field mode quantization in a cavity [15]. Entanglement of mesoscopic states of the electromagnetic field and an atom in a cavity has also been demonstrated [16] in accordance with theoretical considerations (see e.g. Ref. [17]). Even though our analysis will focus on the dynamics of the micromaser we observe that the JC model with damping effects included has been realized in ion traps [18] and in superconducting systems [19]. The coupling of electromagnetic modes to the latter artificial two-level systems has been demonstrated in the laboratory [20, 21]. We also notice that it has experimentally been verified that phonons can be confined in semiconductor planar cavities [22]. It is therefore not unlikely that the present analysis may find applications in systems similar to the micromaser system but realized in a completely different physical framework.

The paper is organized as follows. In Section II we outline the dynamics of a typical experimental setup of the two-level system interacting with a single-mode of the radiation field. Long-time correlations are discussed in Section III and corrections due to detection efficiencies are discussed in Section IV. Collective effects due to the finite probability of having two atoms at a time in the cavity are analyzed in Section V together with possible effects on the detection of trapping states. In Section VI we summarize our work and indicate effects on the phase transitions of the micromaser system in the so called large- N limit.

II. MICROMASER DYNAMICS

In our analysis we consider the following typical realization of the micromaser. The pump atoms which enter the cavity are at resonance with the radiation field of the cavity, and are also assumed to be prepared in the excited state. The injection intervals between the incoming

[†]Permanent address

*Electronic address: boskag@phys.ntnu.no

atoms are assumed to be Poisson-distributed. In terms of the dimensionless atomic flux parameter $N = R/\gamma$, where R is the rate injected atoms and γ is the damping rate of the cavity, the stationary photon number probability distribution is then described by a diagonal density matrix with diagonal elements which are well known [8] and are given by

$$\bar{p}_n = \bar{p}_0 \prod_{m=1}^n \frac{n_b m + N q_m}{(1 + n_b) m} . \quad (1)$$

Here $q_m \equiv q(x) = \sin^2(\theta\sqrt{x})$, with $x = m/N$, and where we have defined the natural dimensionless pump parameter $\theta = g\tau\sqrt{N}$ in terms of the atomic transit time τ . Furthermore, g is the single photon Rabi frequency at zero detuning of the JC-model [13]. The overall constant \bar{p}_0 is determined by $\sum_{n=0}^{\infty} \bar{p}_n = 1$.

The theory as developed in Refs.[8, 23] suggests the existence of various phase transitions in the large- N limit as the parameter θ is increased. A natural order parameter is then the average photon ‘‘density’’ $\langle x \rangle$, where $\langle \cdot \rangle$ denotes an average with respect to the distribution Eq. (1). An exact large- N limit treatment of the micromaser phases structure and the corresponding critical fluctuations in terms of a conventional correlation length was presented in Refs.[24]. Spontaneous jumps in $\langle n \rangle/N$ and large correlation lengths close to micromaser phase transitions have actually been observed experimentally [1, 25]. Several new intriguing physical properties of the micromaser system are unfolded when the theoretical analysis is extended to a more general setup of the parameters available in the micromaser system than those considered here [26].

III. LONG-TIME CORRELATION EFFECTS

Let us now consider long-time correlations in the large- N limit as was first introduced in Refs.[24]. These correlations are most conveniently expressed in terms of the continuous-time formulation of the micromaser system [27]. The vector p formed by the diagonal density matrix elements of the photon field then obeys the differential equation

$$\frac{dp}{dt} = -\gamma L p , \quad (2)$$

where $L = L_C - N(M - 1)$. Here L_C describes the damping of the cavity, i.e.

$$(L_C)_{nm} = (n_b + 1)[n\delta_{n,m} - (n + 1)\delta_{n+1,m}] + n_b[(n + 1)\delta_{n,m} - n\delta_{n,m+1}] , \quad (3)$$

and $M = M(+) + M(-)$, where $M(+)_nm = (1 - q_{n+1})\delta_{n,m}$ and $M(-)_nm = q_n\delta_{n,m+1}$ have their origin in

the JC-model [13, 24]. The lowest eigenvalue $\lambda_0 = 0$ of L then determines the stationary equilibrium solution $\bar{p} = p^{(0)}$ as given by Eq. (1). $\mathcal{P}_s(\tau) = \text{Tr}[M(+)\bar{\rho}] = \bar{u}^T M(s)\bar{p}$ then is the probability that an atom is found in the state $s = \pm$, where $+$ ($-$) denotes the excited(ground) state, after it leaves the microcavity. The vector \bar{u}^T is the transpose of the vector \bar{u} with all entries equal to 1. Here we have used the fact that the vector \bar{u}^T simply represents the trace operation and $\bar{\rho}$ is the diagonal density matrix of the cavity field. When the injection intervals between the incoming atoms are Poisson-distributed, as we have assumed is the case, the joint probability, $\mathcal{P}(s_1, s_2, t)$, of observing two atoms in the states s_1 and s_2 with a large time delay t between them can be written in the form

$$\begin{aligned} \mathcal{P}(s_1, s_2, t) &= \text{Tr}[S(s_2) e^{-\gamma L t} S(s_1)\bar{\rho}] \\ &= \bar{u}^T M(s_2) e^{-\gamma L t} S(s_1) \bar{p} . \end{aligned} \quad (4)$$

The time delay t corresponds to a large number, $k \simeq Rt$, of unobserved atoms between the two detections. In Eq.(4) we make use of the propagation matrix

$$S(s) = (1 + L_C/N)^{-1} M(s) , \quad (5)$$

where $S = S(+) + S(-)$. S is a so called stochastic matrix (see e.g. Refs.[28, 29]) with left ($u_S^{(n)}$) and right ($p_S^{(n)}$) eigenvectors corresponding to the eigenvalue κ_n , where $n = 0, 1, 2, \dots$, such that $1 = \kappa_0 > \kappa_1 > \dots \geq 0$. The stationary distribution as given by Eq.(1) corresponds to the eigenvalue $\kappa_0 = 1$, i.e. $u_S^{(0)} = \bar{u}$ and $p_S^{(0)} = \bar{p}$. The spectral decomposition of S^k , where $k = 0, 1, \dots$, i.e.

$$S^k = \sum_{n=0}^{\infty} \kappa_n^k p_S^{(n)} u_S^{(n)T} , \quad (6)$$

is useful in many of the numerical calculations presented below. Here the normalization is such that $u_S^{(n)T} p_S^{(m)} = \delta_{nm}$. The joint probability $\mathcal{P}(s_1, s_2, t)$ is symmetric, i.e. $\mathcal{P}(s_1, s_2, t) = \mathcal{P}(s_2, s_1, t)$, and is properly normalized, i.e. $\sum_{s_1, s_2} \mathcal{P}(s_1, s_2, t) = 1$ since $S\bar{p} = \bar{p}$ and $\bar{u}^T \bar{p} = 1$. In the original discrete formulation of the micromaser system [8] the corresponding joint probability $\mathcal{P}_k(s_1, s_2)$ of observing two atoms in the states s_1 and s_2 , with k unobserved atoms between, can be written in the form

$$\mathcal{P}_k(s_1, s_2) = \text{Tr}[S(s_2) S^k S(s_1)\bar{\rho}] = \bar{u}^T M(s_2) S^k S(s_1) \bar{p} . \quad (7)$$

This joint probability is also properly normalized, i.e. $\sum_{s_1, s_2} \mathcal{P}_k(s_1, s_2) = 1$. For a sufficiently large k and with $k \simeq Rt$ it now follows that

$$\mathcal{P}_k(s_1, s_2) = \bar{u}^T S(s_2) e^{-\gamma L t} S(s_1) \bar{p} = \mathcal{P}(s_1, s_2, t) \quad (8)$$

in the large- N limit [24] and where L is as in Eq. (2). A formal way to see the validity of Eq.(8) is to notice that $(1 + L_C/N)^{-1} = 1 - L_C/N + \mathcal{O}(1/N^2)$. We can then write

$$S = 1 - \frac{1}{N}(L_C - N(M - 1)) , \quad (9)$$

apart from terms of order $L_C(M-1)/N$ and higher orders in $1/N$. Below we will find expansions of the form Eq.(9) very useful in the analysis of detection efficiencies. We observe that the joint probabilities $\mathcal{P}_k(s_1, s_2)$ are symmetric in s_1 and s_2 [24] as in the continuous-time formulation, i.e. the order in which the atoms are measured is irrelevant. Other definitions for such joint probabilities have appeared in the literature. In the definition for the two-time coincidence probability used in e.g. Refs.[30, 31], $S(s_1)$ in Eqs. (4) and (7) is replaced by $M(s_1)$. With the Poisson-statistics assumption behind the derivation of these equations this would, however, seem like an unnatural thing to do. Since the correlation length to be defined and used below is only sensitive to the eigenvalues of the operator L , our discussions below will not, in the end, be effected by such a modification, at least not in the large- N limit. With detector efficiencies η_+ and η_- for detecting atoms in the excited or ground state respectively, the sequence probabilities defined and used in Ref.[33] are identical to our joint probabilities Eq.(7) in the discrete formulation of the micromaser if $\eta_+ = \eta_- = 100\%$. For $k = 0$ the joint probability $\mathcal{P}_k(s_1, s_2)$ reduces to $\mathcal{P}_{s_1 s_2}(\tau)$, i.e. the probability that the next atom is in the state $s_2 = \pm$ if the previous atom has been found in the state s_1 . $\mathcal{P}_{s_1}(\tau)$ exhibits the experimentally observed revivals in microcavity systems [14, 15] and in e.g. ion-traps [18]. $\mathcal{P}_{s_1 s_2}(\tau)$ exhibits in addition so called pre-revivals [24].

A properly normalized correlation function $\gamma_C(t)$ can now be defined and expressed in different but equivalent manners, i.e.

$$\begin{aligned} \gamma_C(t) &\equiv \frac{\langle ss \rangle_t - \langle s \rangle^2}{1 - \langle s \rangle^2} = \frac{\mathcal{P}(+, +, t) - \mathcal{P}(+)^2}{\mathcal{P}(+)\mathcal{P}(-)} \\ &= \frac{\mathcal{P}(-, -, t) - \mathcal{P}(-)^2}{\mathcal{P}(+)\mathcal{P}(-)} = \frac{\mathcal{P}(+)\mathcal{P}(-) - \mathcal{P}(+, -, t)}{\mathcal{P}(+)\mathcal{P}(-)}, \end{aligned} \quad (10)$$

where $\langle ss \rangle_t = \sum_{s_1, s_2} s_1 s_2 \mathcal{P}(s_1, s_2, t)$ and $\langle s \rangle = \sum_s s \mathcal{P}(s)$. This correlation function satisfies $-1 \leq \gamma_C(t) \leq 1$. At large times $t \rightarrow \infty$, we then define the atomic beam correlation length ξ_C by [24]

$$\gamma_C(t) = \gamma_C e^{-t/\xi_C}, \quad (11)$$

which then is determined by the next-to-lowest eigenvalue λ_1 of L , i.e. $\gamma_C \xi_C = 1/\lambda_1$. In the discrete formulation of the micromaser system we make the replacement $\mathcal{P}(s_1, s_2, t) \rightarrow \mathcal{P}_k(s_1, s_2)$ in Eq.(10) and, for a sufficiently large k , we then define, in a similar manner, the correlation length ξ_D by the expression

$$\gamma_D(k) = \gamma_D e^{-k/R\xi_D}. \quad (12)$$

In the large- N limit one can show that ξ_C and ξ_D converge to the same limit and we therefore write $\xi \equiv \xi_C = \xi_D$ for sufficiently large N [24]. For photons a similar analysis leads us to a correlation length ξ_γ . It follows that the correlation lengths so defined are identical in

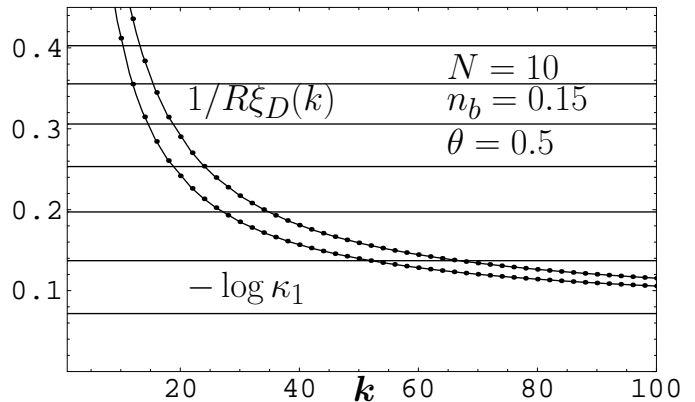


FIG. 1: The convergence of the correlation length $1/R\xi_D(k) = -\log(|\gamma_D(k)|)/k$ as a function of the number $k \simeq Rt$ of unobserved atoms leaving the cavity for $\theta = 0.5$, $N = 10$ and $n_b = 0.15$ in the case of the discrete formulation of the micromaser system with an analytical fit using only the next to the leading eigenvalue κ_1 of the stochastic matrix S as defined in the main text. The corresponding correlation length is $R\xi \approx 14$. The upper curve corresponds to the definition of joint probabilities of the present paper. The lower curve corresponds to a redefinition $S(s_1) \rightarrow M(s_1)$ in the joint probabilities Eq.(7). The horizontal lines corresponds $-\log(\kappa_n)$ for $n = 1, \dots, 7$.

the large- N limit, i.e. $\xi_\gamma = \xi$ [24]. In Fig. 1 we illustrated the convergence of $1/R\xi_D(k) \equiv -\log(|\gamma_D(k)|)/k$ to its asymptotic value $1/R\xi = -\log(\kappa_1)$ for a typical experimental setup of the micromaser system. We observe that spectral resolution Eq.(6) and the definition Eq.(10) modified to yield $\gamma_D(k)$ leads to

$$\gamma_D(k) = \sum_{n=1}^{\infty} c_n \exp(-k \log(1/\kappa_n)) \quad , \quad (13)$$

where we have defined

$$\begin{aligned} c_n &= \sum_{s_1 s_2} \frac{\bar{u}^T M(s_1) p_S^{(n)} u_S^{(n)T} S(s_2) \bar{p}}{1 - \langle s \rangle^2} \\ &= \frac{\bar{u}^T M(+) p_S^{(n)} u_S^{(n)T} S(+) \bar{p}}{\mathcal{P}_+ \mathcal{P}_-} \quad . \end{aligned} \quad (14)$$

The analytical fits in Fig.1, $1/R\xi_D = c_1/k - \log(\kappa_1)$, are based on using only the $n = 1$ term in Eq.(13). We have found that this approximation works for all θ despite the fact that N is small in this case. The numerical value of c_1 can easily be computed numerically given the micromaser parameters. The upper curve in Fig.1 corresponds to the definition Eq.(7) of joint probabilities and leads to $c_1 \approx 3.40$. The lower curve in Fig. 1 corresponds to a redefinition $S(s_1) \rightarrow M(s_1)$ in the joint probabilities

Eq.(7) and leads to $c_1 \approx 4.37$. In Fig.2 we compare the correlation length $\gamma\xi$ using the discrete and continuous-time formulation of the micromaser system for a typical setup of parameters. We observe the rapid convergence of the two formalisms already for a small value of N . In the sequel we will therefore make use of the fact that $\gamma\xi = 1/\lambda_1 = 1/N \log(1/\kappa_1)$ if N is large enough.

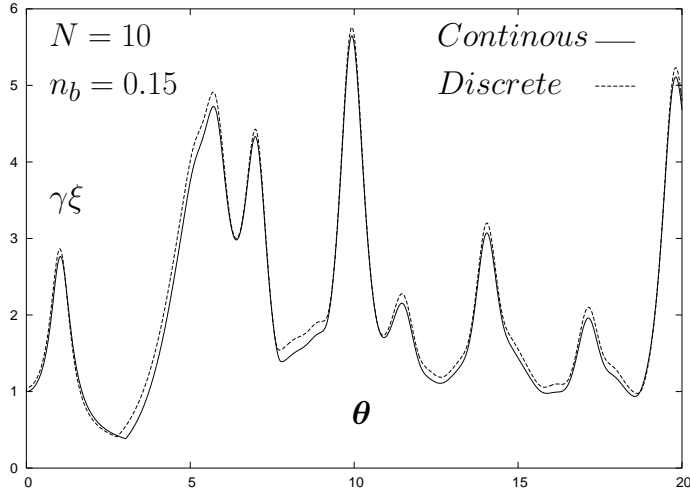


FIG. 2: The correlation length $\gamma\xi$ as a function of θ for $N = 10$ and $n_b = 0.15$ in the case of the continuous-time (solid line) and the discrete (dashed line) formulation of the micromaser system as described in the main text.

IV. DETECTION EFFICIENCIES

It has been emphasized in the literature that in the analysis of the micromaser system, when detection efficiencies has to be taken into account, one must distinguish between the occurrence of a certain detection event and the absence of such a detection event. This is so since the detection of an atom leaving the cavity necessarily gives rise to an instantaneous and non-local state reduction of the micromaser cavity radiation field. In Refs.[32] a non-linear equation of motion was derived taking such effects into account. In studying the statistics of sequence events it was, however, shown in Ref.[30] that one may make use of a linear equation of motion for non-normalized states. Recently it has been shown in detail how these different formalisms actually leads to the same physical results [33]. Below we follow the analysis of Refs.[30, 33] since we find it simpler to implement numerically.

Our calculation of joint or sequence probabilities when detection efficiencies must be taken into account follows

the scheme outlined in Ref.[33]. There is simple prescription how to modify the analysis in Section III to the situation with, in general, different detection efficiencies η_+ and η_- . The basic matrices $M(\pm)$ are naturally modified to $\bar{M}(s) = \eta_s M(s)$ with $s = \pm$ and we therefore also modify $M = M(+) + M(-)$ to $\bar{M} = \eta_+ M(+) + \eta_- M(-)$. It is also convenient to define the matrix $\bar{M}_- = \bar{M} - M$. It then follows that the joint probability as given by Eq.(7) is modified according to

$$\mathcal{P}_k(s_1, s_2) \rightarrow \bar{\mathcal{P}}_k(s_1, s_2) = \bar{u}^T \bar{M}(s_2) \bar{S}^k \bar{S}(s_1) \bar{p} / \mathcal{N} \quad , \quad (15)$$

where we have defined the matrix

$$\bar{S}(s) = (1 + L_C/N + \bar{M}_-)^{-1} \bar{M}(s) \quad . \quad (16)$$

Here $\bar{S} = \bar{S}_+ + \bar{S}_-$ and $\mathcal{N} = \eta_+ \mathcal{P}_+ + \eta_- \mathcal{P}_-$ is a normalization factor. We also make the modification $\mathcal{P}(s) \rightarrow \bar{\mathcal{P}}(s) = \eta_s \mathcal{P}(s) / \mathcal{N}$. It is of importance to observe that the stationary micromaser photon number distribution Eq.(1) still can be obtained from the stationary condition $\bar{S}\bar{p} = \bar{p}$. The discussions in Section III in the case of the discrete formulation of the micromaser system can now simply be carried through by changing the relevant probabilities by the modified probabilities defined above and one, e.g., shows that $\bar{\mathcal{P}}_k(s_1, s_2) = \bar{\mathcal{P}}_k(s_2, s_1)$, which was shown explicitly for $k = 0$ in Ref.[33]. We therefore define the correlation function

$$\begin{aligned} \bar{\gamma}_D(k) &= \frac{\bar{\mathcal{P}}(+)\bar{\mathcal{P}}(-) - \bar{\mathcal{P}}_k(+, -)}{\bar{\mathcal{P}}(+)\bar{\mathcal{P}}(-)} \\ &= \bar{\gamma}_D e^{-k/R\bar{\xi}_D} \quad , \end{aligned} \quad (17)$$

expressed in one of many equivalent manners as in Eq.(17). For N large enough we can then write $\xi = \bar{\xi}_D$ if $\eta_+ = \eta_- = 1$. Using a $1/N$ expansion similar to Eq.(9) we now find that

$$\bar{S} = 1 - \frac{1}{N}(L_C - N\bar{M}_-) + (\bar{M} - 1) = S \quad , \quad (18)$$

apart from higher order terms in $(L_C - N\bar{M}_-)/N$ and higher orders in $1/N$. For sufficiently large N we would then e.g. conclude that

$$\bar{\mathcal{P}}_k(s_1, s_2) = \bar{u}^T \bar{M}(s_2) e^{-\gamma L t} \bar{S}(s_1) \bar{p} / \mathcal{N} \quad . \quad (19)$$

The correlation length $\bar{\xi} \equiv \bar{\xi}_D$ in Eq.(17) would then again be determined by the next-to-lowest eigenvalue of L and, as a result, $\bar{\xi}$ would actually not depend on the detection efficiencies at all and therefore equal to ξ . This was the claim as announced in Refs.[26]. This conclusion is basically correct apart from a trivial correction which, unfortunately, was not taken into account. The physical explanation of this correction is simply the fact that the time interval t in Eq.(19) should be such that Rt is average number of atoms which the observer claims passes through the micromaser system, i.e. $Rt \simeq k(\eta_+ \mathcal{P}(+) + \eta_- \mathcal{P}(-))$ and not $Rt \simeq k$. This means that the correlation length ξ is "renormalized" to

$\bar{\xi} = (\eta_+ \mathcal{P}(+) + \eta_- \mathcal{P}(-))\xi$. A more formal proof of this assertion can be given as follows. Let us first consider the case of equal detection efficiencies, i.e. $\eta \equiv \eta_+ = \eta_-$. Since the correlation length $\bar{\xi}$ will be determined by the next-to-leading eigenvalue $\bar{\kappa}_1$ of the operator \bar{S} , i.e. $\gamma\bar{\xi} = 1/N \log(1/\bar{\kappa}_1)$ for large N , we study the eigenvalue problem $\bar{S}\bar{p}_D = \bar{\kappa}\bar{p}_D$. As in Ref.[24] it is convenient to rewrite such an eigenvalue problem in an equivalent form, i.e.

$$\left(L_C - N\left(1 + \frac{\eta}{\bar{\kappa}} - \eta\right)(M - 1) \right) \bar{p}_D = \eta N \left(\frac{1}{\bar{\kappa}} - 1 \right) \bar{p}_D \quad . \quad (20)$$

This equation can now be compared to the eigenvalue problem in the case of the continuous-time formulation of the micromaser system with $\eta_+ = \eta_- = 1$, i.e.

$$(L_C - N(M - 1)) p_C = \lambda(N) p_C \quad , \quad (21)$$

where we have made the N dependence explicit in the eigenvalue $\lambda(N)$. By comparing Eqs.(20) and (21) we conclude that

$$\lambda \left(N \left(1 + \frac{\eta}{\bar{\kappa}} - \eta \right) \right) = \eta N \left(\frac{1}{\bar{\kappa}} - 1 \right) \quad . \quad (22)$$

Since $\lambda(N)$ remains finite in the large- N limit, we can write $\lambda(N(1 + \eta/\bar{\kappa} - \eta)) \rightarrow \lambda(N)$ for sufficiently large N and we conclude that

$$\frac{1}{\bar{\kappa}_1} = 1 + \frac{\lambda_1}{\eta N} = 1 + \frac{1}{\eta \gamma \xi N} \quad . \quad (23)$$

We therefore find that $\gamma\bar{\xi} = \eta\gamma\xi$ apart from $1/N$ corrections. A consequence of this analysis is that $\eta N(1/\bar{\kappa} - 1)M\bar{p}_D = \eta N(1/\bar{\kappa} - 1)\bar{p}_D$ in the large- N limit as can be seen again by comparing Eqs.(20) and (21). This can be understood as follows. For large N the components eigenvector \bar{p}_D will be distributed around some large component. We can then replace the matrices $M(s)$ for $s = \pm$ by the diagonal matrices $\mathcal{P}(s)$, i.e. their mean-field values, in the expression $\eta N(1/\bar{\kappa} - 1)M\bar{p}_D$ above. Extending the analysis above for a equal detection efficiencies to the case with different ones, we then find that $\gamma\bar{\xi} = (\eta_+ \mathcal{P}(+) + \eta_- \mathcal{P}(-))\gamma\xi$ apart from $1/N$ corrections. Numerically, it turns out that the convergence of the correlation length as a function of N is very rapid. In Figs. 3 we study, as an example, the correlation length $\gamma\xi \equiv \gamma\xi_D$ for a moderate value of $N = 10$ and other parameters adapted to experimental data on trapping effects in the micromaser system [10]. One verifies that $\gamma\bar{\xi}(\theta = 0) = (N \log(1 + 1/N\eta_+))^{-1}$ in excellent agreement with numerical simulations in general. We find it remarkable that the scaling law for detection efficiencies of the ratio of correlation lengths $\bar{\xi}/\xi = \eta_+ \mathcal{P}(+) + \eta_- \mathcal{P}(-)$ works so well for such a small value of N as used in e.g. Figs.3. Experimentally one could therefore measure the appropriate sequence probabilities, evaluate the correlation length and then renormalize the corresponding data with an easily calculable factor. The resulting correlation

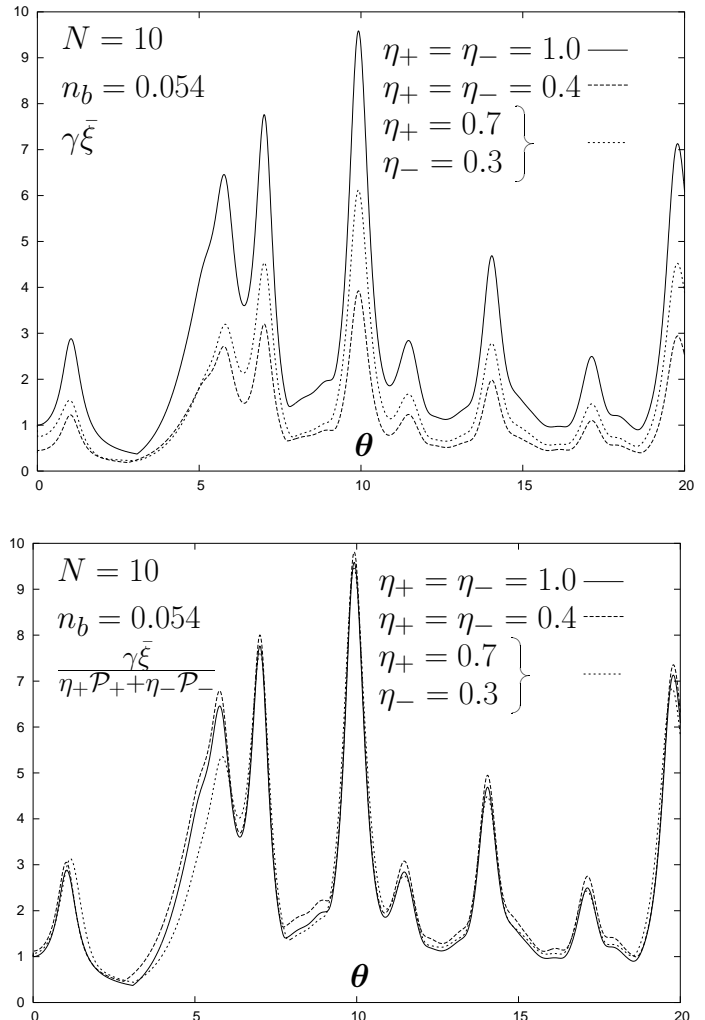


FIG. 3: In the upper graph the correlation length $\gamma\bar{\xi}$ is given as a function of θ for $N = 10$ and $n_b = 0.054$ for various values of detection efficiencies. With equal detection efficiencies $\eta = \eta_+ = \eta_-$ (lower curve) the correlation length is given by $\eta\gamma\xi$ with $\xi = \bar{\xi}(\eta_+ = \eta_- = 1)$. In the lower graph we consider the same parameters but a "renormalized" correlation $\gamma\bar{\xi}/(\eta_+ \mathcal{P}_+ + \eta_- \mathcal{P}_-)$.

length so obtained is then the one that was predicted in Refs.[24].

V. COLLECTIVE EFFECTS

Collective effects are now due to the fact that during a time interval t , such that $0 < t < \tau$, two atoms has

jointly interacted with the same cavity radiation field. An ideal and very special situation corresponds $t = \tau$ which has been discussed in great detail in Ref.[34] and also elsewhere [35]. The general situation is more tedious but straightforward to analyze and has been discussed in great detail in Ref.[36] in terms of an expansion in the parameter $\epsilon = R\tau$. This parameter is supposed to be small, i.e. $\epsilon \ll 1$, in order to be close to the one-atom maser situation (see e.g. Appendix A in the second reference of Ref.[24]). We have reconsidered the analysis of Ref.[36]. The generator L in the master equation Eq.(2) is, up to first order terms in ϵ , modified according to

$$\begin{aligned} \frac{dp}{dt} = & -\gamma(L_C - (1 - 2\epsilon)N(M - 1))p \quad , \\ & + \gamma N \frac{\epsilon}{\tau} \int_0^\tau dt u_2(t)p \quad , \end{aligned} \quad (24)$$

where the two-atom generator $u_2(t)$ describes two atoms that have jointly interacted with the cavity during the time interval t such that $0 < t < \tau$ and given explicitly in Ref.[36]. One finds that the generator L in the master equation Eq.(2) is replaced by $L_{tot} = L + L_{col}$, where L_{col} describes the two-atom collective effects with matrix elements given by

$$\begin{aligned} (L_{col})_{nm} = & N\epsilon[(w_n(\tau) + v_n(\tau))\delta_{n,m} \\ & - v_{n-1}(\tau)\delta_{n,m+1} - w_{n-2}(\tau)\delta_{n,m+2}] \quad . \end{aligned} \quad (25)$$

Here we have defined

$$\begin{aligned} v_n(\tau) = & \frac{1}{\tau} \int_0^\tau dt \left([q_{n+1}(\tau - t) + b_n(t)][1 - q_{n+1}(\tau - t) \right. \\ & - q_{n+2}(\tau - t)] - q_{n+1}(\tau)[1 - q_{n+1}(\tau) - q_{n+2}(\tau)] \\ & \left. - [c_n(t) + d_n(t)][q_{n+1}(\tau - t) - q_{n+2}(\tau - t)] \right) \quad , \end{aligned} \quad (26)$$

and

$$\begin{aligned} w_n(\tau) = & \frac{1}{\tau} \int_0^\tau dt \left(c_n(t) + q_{n+2}(\tau - t)q_{n+1}(\tau - t) \right. \\ & \left. + b_n(t)q_{n+2}(\tau - t) + [c_n(t) + d_n(t)]q_{n+2}(\tau - t) \right) \quad . \end{aligned} \quad (27)$$

In these definitions we make use of the functions $q_n(t) \equiv q_n = \sin^2(gt\sqrt{n})$,

$$\begin{aligned} b_n(t) = & \frac{n+1}{2n+3}q_{n+3/2}(2t)[1 - q_{n+1}(\tau - t)] \\ & - \frac{1}{2}q_{n+3/2}(2t)q_{n+1}(\tau - t) \quad , \end{aligned} \quad (28)$$

and

$$\begin{aligned} c_n(t) = & \frac{n+1}{2(2n+3)}q_{n+3/2}(2t)[1 - q_{n+1}(\tau - t)] \\ & + q_{n+3/2}^2(t)q_{n+1}(\tau - t) \quad , \end{aligned} \quad (29)$$

and, finally,

$$\begin{aligned} d_n(t) = & 4 \frac{n+1}{2n+3} \frac{n+2}{2n+3} q_{n+3/2}^2(t)[1 - q_{n+1}(\tau - t)] \\ & + \frac{n+2}{2(2n+3)} q_{n+3/2}(2t)q_{n+1}(\tau - t) \quad . \end{aligned} \quad (30)$$

Our final expression for L_{tot} is, in fact, in agreement with

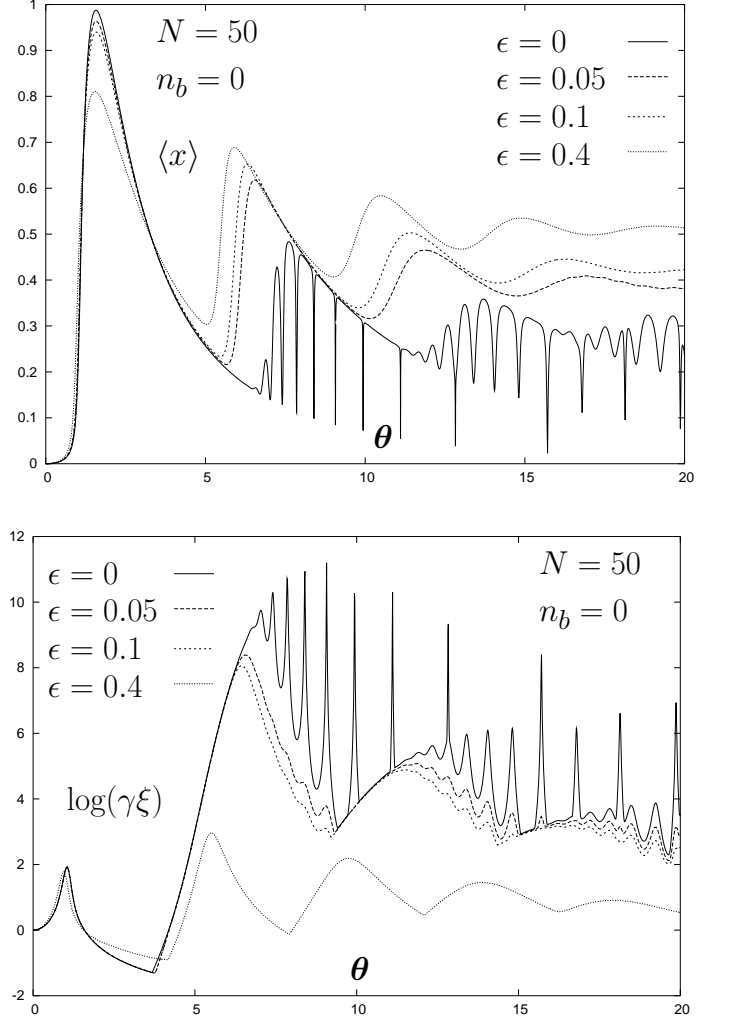


FIG. 4: In the upper graph the order parameter $\langle x \rangle = \langle n/N \rangle$ is given as a function of θ for $N = 50$ and $n_b = 0$ for various values of $\epsilon = R\tau$. It is only for $\epsilon = 0$ that trapping-state peaks are visible. In the lower graph the correlation length $\gamma\xi$ is given for the same set of parameters. Even though the trapping-state peaks vanishes as ϵ increases, the correlation length can still be large for $\epsilon \neq 0$. The peaks at $\theta \simeq 10$ correspond to the first maser transition.

the result of Ref.[36] using a slightly different notation. It is rather straightforward to implement the matrix elements of L_{tot} in a numerical routine in order to find

the new stationary distribution \bar{p} corresponding to the eigenvalue $\lambda_0 = 0$ of L_{tot} to be used in evaluating various expectation values. The correlation length is again determined by the next-to-lowest eigenvalue λ_1 of L_{tot} . In the numerical work it turns out to be sufficient to use 200x200 matrices for both L and L_{tot} in order to obtain the accuracy of the graphs as presented in the present paper. In Fig.4 we show the results of a numerical evaluation of the order parameter $\langle x \rangle$ and the correlation length $\gamma\xi$ for $N = 50$ in a vacuum configuration ($n_b = 0$).

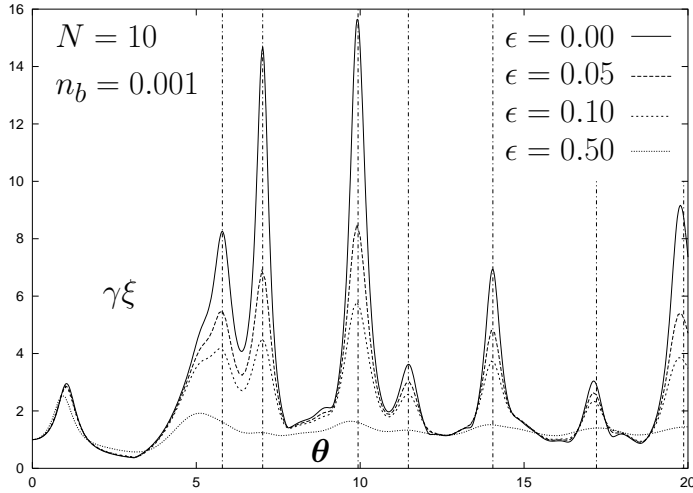


FIG. 5: The correlation length $\gamma\xi$ as a function of θ for various values of ϵ . The vertical lines indicate the trapings values of $\theta = \pi\sqrt{N}(1/\sqrt{3}, 1/\sqrt{2}, 1, 2/\sqrt{3}, \sqrt{2}, \sqrt{3}, 2)$.

Our results basically agree with the corresponding numerical results of Ref.[36] even though we apparently have a higher numerical precision. As argued in Ref.[36], effects of trapping states at $\theta = k\pi\sqrt{N/n}$, for $k, n = 1, 2, \dots$, vanishes as $\epsilon \neq 0$. This is, however, not so for the correlation length $\gamma\xi$ as indicated in the lower figure of Fig.4. In fact, if we consider even a lower value of $N = 10$ and $n_b = 0.001$ as in Fig.5, trapping-state effects are clearly seen in the correlation length. In Fig.5 the vertical lines corresponds to the clearly visible trapping states with $\epsilon = 0$. In the experimental study of trapping-states in Ref.[10] the parameters are, however, varied in such a way that the parameter ϵ is not constant but is given by $\epsilon = R\tau = \theta\sqrt{N}\gamma/g$ as in Fig.6, where we have chosen the cavity temperature to be $T = 0.3K$, corresponding to $n_b = 0.054$. The average photon lifetime in the cavity corresponding to Fig.6 is 0.1 s, i.e. $\gamma = 10 s^{-1}$. The vertical lines in Fig.6 correspond to the trapping-states as considered in Ref.[10] and studied in terms of the atomic inversion. With detection efficiencies taken into account, the appropriate definition of the

atom inversion $I(\tau)$ is given by

$$I(\tau) = \frac{\eta_+\mathcal{P}(+) - \eta_-\mathcal{P}(-)}{\mathcal{N}} = \frac{(\eta_+ + \eta_-)n_b}{\mathcal{N}} - \frac{\eta_+ + \eta_-}{\mathcal{N}}\langle x \rangle, \quad (31)$$

where \mathcal{N} is the normalization factor $\eta_+\mathcal{P}(+) + \eta_-\mathcal{P}(-)$. Eq.(31) gives the general relation between the atomic inversion $I(\tau)$ and the order parameter $\langle x \rangle$. We observe that if $\eta \equiv \eta_+ = \eta_-$ then $I(\tau)$ is independent of η . It is clear from our Fig.6 that trapping effects are much more visible in the correlation length than in the order parameter $\langle x \rangle$. It is also clear that collective effects are small with the set of micromaser parameters chosen. Instead detection efficiency will be a major correction to the theoretical values. In Section IV we have seen how the correlation length is to be corrected for due to detection efficiencies. In view of these results it therefore appears that trapping-states can be more clearly revealed experimentally in terms of the correlation length rather than the atomic inversions or, equivalently, the order parameter $\langle x \rangle$.

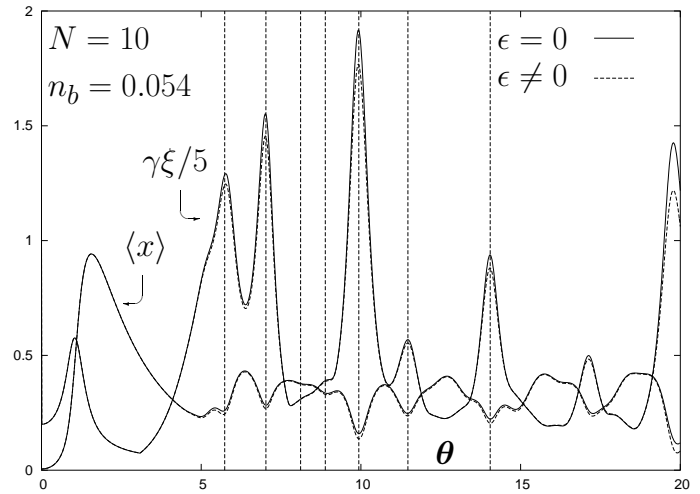


FIG. 6: The order parameter $\langle x \rangle$ and the correlation length $\gamma\xi/5$ as a function of θ with no collective effects taken into account ($\epsilon = 0$) or $\epsilon = R\tau = \theta\sqrt{N}\gamma/g$. The Rabi frequency is as in the experimental study of trapping-states in Ref.[10], i.e. $g = 39 kHz$ and $\gamma = 10 s^{-1}$. The vertical lines indicate the experimentally observed trapings values of $\theta = \pi\sqrt{N}(1/\sqrt{3}, 1/\sqrt{2}, 2/\sqrt{6}, 2/\sqrt{5}, 1, 2/\sqrt{3}, \sqrt{2})$ as reported in Ref.[10].

VI. FINAL REMARKS

In conclusion, we have studied how to take detection efficiencies into account when comparing experimental data for the correlation length to the theoretical predictions. We have found a remarkable and simple scaling relation that connects observational data and the theoretical prediction. We have also studied two-atom collective effects in terms of the natural parameter $\epsilon = R\tau$. Even though cumbersome, the calculations are in principle straightforward. Trapping effects appear to be suppressed with increasing values of ϵ . We have, however, seen that in a realistic experimental situation, as discussed in e.g. Ref.[10], collective effects are, nevertheless, small and detection efficiencies are more important to take into account. As we have shown, detection efficiencies can, however, be taken into account in a straightforward manner.

With increasing values of N , signals due to the micromaser phase transitions become more pronounced. General methods, which are exact in the large- N limit, for computing characteristic features of these phase transition have been presented in Refs.[24, 26]. Detection efficiencies will only imply a calculable rescaling as discussed in Section IV.

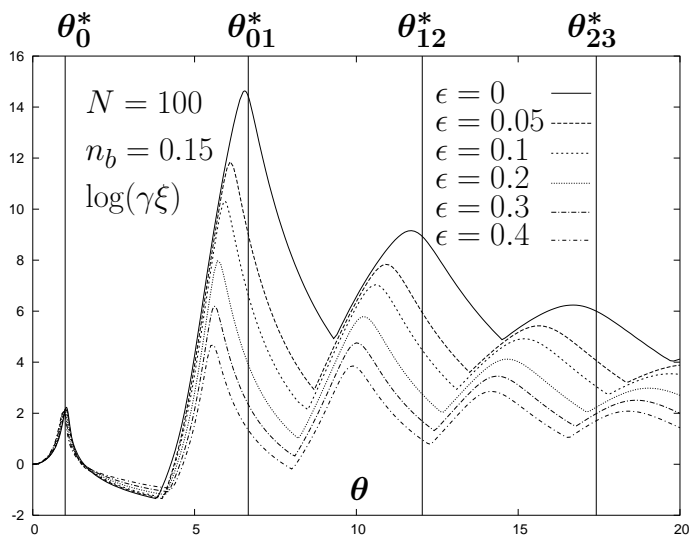


FIG. 7: The correlation length $\gamma\xi$ as a function of θ for various values of ϵ . The vertical lines indicate the large N values for the maser phase transitions at $\theta = \theta_0^* = 1, \theta_{01}^* \approx 6.6610, \theta_{12}^* \approx 12.035, \theta_{23}^* \approx 17.413$. With $\langle x \rangle$ as an order parameter, the transition at $\theta = \theta_0^*$ is second order while the other are first order transitions.

Due to the random arrival statistics of the pump atoms

there is, however, in an actual experimental situation a finite probability of more than one pump atom in the cavity [34]. Since the average number of pump atoms inside the cavity is $\epsilon \equiv \tau R = \gamma\sqrt{N}\theta/g$, this parameter, as we have seen above, naturally parameterize the probability of collective pump atom effects. If ϵ is assumed to be constant and small, i.e. $\epsilon \ll 1$, we see that the dimensionless pump parameter N is bounded by $\sqrt{N} \ll g/\gamma\theta$. Arbitrarily large values of N can then only be reached by making g/γ arbitrarily large which, of course, is difficult to achieve in a real experimental realization of the micromaser. Alternative $\epsilon = \theta\sqrt{N}g/\gamma$ should be small as θ varies. As we have seen in the present paper, if ϵ is sufficiently small, corrections to the observables as discussed in the present paper can be calculated in a rather straightforward manner.

At finite N and including collective pump atom effects, signals of the large N phase transitions in the order parameter $\langle x \rangle$ are still clearly exhibited, at least in the case when the pump atoms are prepared in the excited state and at resonance with cavity radiation field. The critical point θ_0^* of the first second-order maser transition remains the same with $\langle x \rangle$ used as a natural order parameter. As seen from Eq.(24) when taking collective effects into account for a sufficiently small ϵ , one-atom effects are modified by a renormalization $N \rightarrow \exp(-2\epsilon)N$, where $\exp(-2\epsilon) \approx 1 - 2\epsilon$ is the probability for one-atom events in the micromaser cavity. We therefore expect that the critical parameters $\theta_{kk+1}^* \propto \sqrt{N}$ of first-order transitions are changed to $\bar{\theta}_{kk+1}^* \equiv \exp(-\epsilon)\theta_{kk+1}^*$. By making use of the general results of Refs.[24, 26] concerning the N dependence of the peak values of the correlation length these are changed accordingly, and we find that $\log(\gamma\xi)_{crit}$ is changed to $\log(\gamma\bar{\xi})_{crit} = \exp(-\epsilon)\log(\gamma\xi(\theta = \theta_{kk+1}^*))$. In Fig.7 we illustrate these effects in the case $N = 100$ and $n_b = 0.15$. For small values of ϵ we find that the scaling behavior given above for $\bar{\theta}_{kk+1}^*$ and $\log(\gamma\bar{\xi})_{crit}$ are indeed compatible with the exact results.

As in Ref.[36] we also find that our perturbative methods gives meaningful results even when the expansion parameter ϵ is large. In the present paper we have considered a limited range of micromaser parameters. If atoms and the radiation field are not at resonance one can e.g. extend the results of the present paper by making use of the methods of Ref.[26] and the procedures outlined in the present.

ACKNOWLEDGMENT

The author wishes to thank B. T. H. Varcoe and H. Walther and for discussions and H. Walther for providing a guide to the progress in experimental work over the years. Göran Wendin is acknowledged for hospitality during the completion of this work. NorFA is acknowledged for its support.

- [1] H. Walther, "The Single Atom Maser and the Quantum Electrodynamics in a Cavity", *Physica Scripta* **T23** (1988) 165; "Experiments on Cavity Quantum Electrodynamics" *Phys. Rep.* **219** (1992) 263; "Experiments With Single Atoms in Cavities and Traps" in "Fundamental Problems in Quantum Theory", Eds. D. M. Greenberger and A. Zeilinger, *Ann. N.Y. Acad. Sci.* **755** (1995) 133; "Single Atom Experiments in Cavities and Traps", *Proc. Roy. Soc.* **A454** (1998) 431; "Quantum Optics of a Single Atom", *Laser Physics* **8** (1998) 1; *Physica Scripta* **T76** (1998) 138.
- [2] K. An, J. J. Childs, R. R. Dasari and M. S. Feld, "Micro-laser: A Laser with One Atom in an Optical Resonator", *Phys. Rev. Lett.* **73** (1994) 3375.
- [3] J. McKeever, A. Boca, A. D. Boozer, J. B. Buck and H. J. Kimble "Experimental Realization of a One-Atom Laser in the Regime of Strong Coupling", *Nature* **425** (2003) 268.
- [4] A. Buchleitner and R.N. Mantegna, "Quantum Stochastic Resonance in a Micromaser", *Phys. Rev. Lett.* **80** (1998) 3932.
- [5] A. Maritan and J. R. Banavar, "Chaos, Noise, and Synchronization", *Phys. Rev. Lett.* **72** (1994) 1451; B.-S. Skagerstam in "Applied Field Theory", Eds. Choonkye Lee, Hyunsoo Min and Q-Han Park (Chungbum Publ. House, Seoul, 1999).
- [6] P. K. Rekdal and B.-S. Skagerstam, "Noise and Order in Cavity Quantum Electrodynamics", *Physica* **A305** 404 (2002).
- [7] L. Caiani, L. Casetti, C. Clementi and M. Pettini, "Geometry of Dynamics, Lyapunov Exponents, and Phase Transitions", *Phys. Rev. Lett.* **79** (1997) 4361; L. Casetti, E. G. D. Cohen and M. Pettini, "Topological Origin of the Phase Transition in a Mean-Field Model", *Phys. Rev. Lett.* **82** (1999) 4160.
- [8] D. Filipowicz, J. Javanainen and P. Meystre, "The Microscopic Maser", *Opt. Comm.* **58** (1986) 327, "Theory of a Microscopic Maser" *Phys. Rev.* **A34** (1986) 3077.
- [9] J. J. Slosser and P. Meystre "Tangent and Cotangent States of the Electromagnetic Field", *Phys. Rev. A* **41** (1990) 3867.
- [10] M. Weidinger, B. T. H. Varcoe, R. Heerlein and H. Walther, "Trapping States in the Micromaser", *Phys. Rev. Lett.* **82** (1999) 3795.
- [11] S. Brattke, B. T. H. Varcoe and H. Walther, "Generating Photon Number States On Demand Via Cavity Quantum Electrodynamics", *Phys. Rev. Lett.* **86** (2001) 3534.
- [12] R. H. Dicke, "Coherence in Spontaneous Radiation Processes" *Phys. Rev.* **93**, 99 (1954).
- [13] E. T. Jaynes and F. W. Cummings, "Comparison of Quantum and Semiclassical Radiation Theories with Application to the Beam Maser", *Proc. IEEE* **51** (1963) 89.
- [14] G. Rempe, H. Walther and N. Klein, "Observation of Quantum Collapse and Revival in the One-Atom Maser", *Phys. Rev. Lett.* **58** (1987) 353.
- [15] M. Brune, F. Schmidt-Kaler, A. Maali, J. Dreyer, E. Hagley, J. M. Raimond and S. Haroche, "Quantum Rabi Oscillation: A Direct Test of Field Quantization in a Cavity", *Phys. Rev. Lett.* **76** (1996) 1800.
- [16] A. Auffeves, P. Maioloi, T. Meunier, S. Gleyzes, G. Nogues, M. Brune, J. M. Raimond and S. Haroche, "Entanglement of a Mesoscopic Field with an Atom Induced by Photon Graininess in a Cavity", *Phys. Rev. Lett.* **91** (2003) 230405-1.
- [17] P. K. Rekdal, B.-S. Skagerstam and P. L. Knight, "On the Preparation of Pure States in Resonant Microcavities", *J. Mod. Optics.* **51** (2004) 75.
- [18] D. M. Meekhof, C. Monroe, B. E. King, W. M. Itano and D. J. Wineland, "Generation of Nonclassical Motional States of a Trapped Atom", *Phys. Rev. Lett.* **76** (1996) 1796; "Demonstration of a Fundamental Quantum Logic Gate", *ibid.* **75** (1995) 4714; C. Monroe, D. M. Meekhof, B. E. King and D. J. Wineland, "A "Schrödinger Cat" Superposition State of an Atom", *Science* **272** (1996) 1131; C. J. Myatt, B. E. King, Q. A. Turchette, C. A. Sackett, D. Kielpinski, W. M. Itano, C. Monroe and D.J. Wineland, "Decoherence of Quantum Superpositions Through Coupling to Engineered Reservoirs", *Nature* **403** (2000) 269; B. B. Blinov, D. L. Moehring, L.-M. Duand and C. Monroe, "Observation of Entanglement Between a Single Trapped Atom and a Single Photon", **448** (2004) 153.
- [19] Y. Nakamura, Yu. A. Pashkin and J. S. Tsai, "Coherent Control of Macroscopic Quantum States in a Single-Cooper-Pair Box", *Nature* **398** (1999) 786; D. Vion, A. Aassime, A. Cottet, P. Joyez, H. Pothier, C. Urbina, D. Esteve and M. H. Devoret, "Manipulating the Quantum State of an Electrical Circuit", *Science* **296** (2002) 886.
- [20] I. Chiorescu, P. Bertet, K. Semba, Y. Nakamura, C. J. P. M. Harmans and J. E. Mooij, "Coherent Dynamics of a Flux Qubit Coupled to a Harmonic Oscillator", *Nature* **431** (2004) 159.
- [21] A. Wallraff, D. I. Schuster, A. Blais, L. Frunzio, R.-S. Huang, J. Majer, S. Kumar, S. M. Girvin and R. J. Schoelkopf, "Strong Coupling of a Single Photon to a Superconducting Qubit Using Circuit Quantum Electrodynamics", *Nature* **431**1162 (2004).
- [22] M. Trigo, A. Bruchhausen, A. Fainstein, B. Jusserand and V. Thierry-Mieg, "Confinement of Acoustical Vibrations in a Semiconductor Planar Phonon Cavity", *Phys. Rev. Lett.* **89** 227402-1 (2002).
- [23] A. M. Guzman, P. Meystre and E. M. Wright, "Semiclassical Theory of the Micromaser", *Phys. Rev.* **A40** (1989) 2471.
- [24] P. Elmfors, B. Lautrup and B.-S. Skagerstam, "Correlations as a Handle on the Quantum State of the Micromaser", CERN/TH 95-154 (cond-mat/9506058) and *Physica Scripta* **55** (1997) 724; "Correlations in the Micromaser" *Phys. Rev.* **A54** (1996) 5171.
- [25] O. Benson, G. Raithel and H. Walther, "Quantum Jumps of the Micromaser Field: Dynamic Behavior Close to Phase Transition Points", *Phys. Rev. Lett.* **72** (1994) 3506, *ibid.* **75** (1995) 3446, and "Dynamics of the Micro-maser Field" in "Electron Theory and Quantum Electrodynamics: 100 Years Later", Ed. J. P. Dowling (Plenum Press, New York, 1997).
- [26] P. K. Rekdal and B.-S. Skagerstam, "On the Phase Structure of the Micromaser", *Opt. Comm.* **184** (2000) 195 and quant-ph/9910110; "Theory of the Microscopic Maser Phase Transitions", *Physica* **A 315** (2002) 616.
- [27] L. Lugiato, M. Scully and H. Walther, "Connection Between Microscopic and Macroscopic Maser Theory",

- Phys. Rev. **A36** (1987) 740.
- [28] F.-J. Fritz, B. Huppert and W. Willems, "Stochastische Matrizen" (Springer-Verlag 1979).
- [29] L. E. Reichl, "A Modern Course in Statistical Physics" (2nd Edition, Wiley & Sons, New York, 1998).
- [30] U. Herzog, "Statistics of Photons and De-Excited Atoms in a Micromaser With Poisson Pumping ", Phys. Rev. **A50** (1994) 783; "Micromaser Intensity Correlations and Coincidence Probabilities", Appl. Phys. **B60** (1995) S21.
- [31] B.-G. Englert, M. Löffler, O. Benson, M. Weidinger and H. Walther, "Entangled Atoms in Micromaser Physics ", Fortschr. Phys. **46** (1998) 897.
- [32] H.-J. Briegel, B.-G. Englert, N. Sterpi and H. Walther, "One-Atom Masers: Statistics of Detector Clicks ", Phys. Rev. **A 49** (1994) 2962 and B.-G. Englert, T. Gantsog, A. Schenzle, C. Wagner and H. Walther, "One-Atom Maser: Phase-Sensitive Measurements ", Phys. Rev. **A 53** (1996) 4386.
- [33] D. B. Johnson and W. C. Schieve, "Detection Statistics in the Micromaser", Phys. Rev. **A63** 033808 (2001).
- [34] E. Wehner, R. Seno, N. Sterpi, B.-G. Englert and H. Walther, "Atom Pairs in the Micromaser ", Opt. Commun. **110** (1994) 655.
- [35] M. S. Iqbal, S. Mahmood, M. S. K. Rami and M. S. Zubairy, "Interaction of Two Two-Level Atoms With a Single-Mode Quantized Radiation Field ", J. Opt. Soc. Am. **B 5** (1988) 1312; M. Orzag, R. Ramierz, J. C. Retamal and C. Saavedra, "Quantum Cooperative Effects in the Micromaser ", Phys. Rev. **A 49** (1994) 2933; S. Qamar, A. H. Toor and M. S. Zubairy, "Co-operative Atomic Effects in a Micromaser ", Quantum Semiclass. Opt. **7** (1995) 393.
- [36] M. I. Kolobov and F. Haake, "Collective Effects in the Microlaser ", Phys. Rev. **A55** (1997) 3033.